Method for sensitivity analysis of photonic crystal devices

Georgios Veronis, Robert W. Dutton, and Shanhui Fan

Department of Electrical Engineering, Stanford University, Stanford, California 94305

Received April 19, 2004

We present a new method for sensitivity analysis of photonic crystal devices. The algorithm is based on a finite-difference frequency-domain model and uses the adjoint variable method and perturbation theory techniques. We show that our method is highly efficient and accurate and can be applied to calculation of the sensitivity of transmission parameters of resonant nanophotonic devices. © 2004 Optical Society of America

OCIS codes: 230.3990, 230.4000, 260.2110, 130.3120.

For practical implementations of photonic crystal devices, it is of fundamental importance to determine the sensitivity of the device properties to fabrication-related disorders.[1–5] In principle, the sensitivity can be determined by varying the device parameters in the vicinity of the design point, and by calculating the response functions of the resulting perturbed devices. However, such a direct approach is computationally inefficient, since it requires a full analysis for each variation of the design parameters. Moreover, in practice, it is important to determine the sensitivity with respect to variations of geometrical parameters. In the commonly used finite-difference time-domain method, a variation of the device size by a single grid point may already lead to large structural change. Consequently, to determine the sensitivity accurately in the direct approach, a high-resolution grid is typically needed, further increasing the computational cost.

In this Letter we introduce a new approach for sensitivity analysis of photonic crystal structures based on the adjoint variable method[6] (AVM) and perturbation theory in a frequency-domain solver for Maxwell's equations. In this approach, once a simulation for the device properties is performed, the sensitivity with respect to any number of design parameters is calculated with very small additional computational cost. Furthermore, this approach determines the sensitivity with respect to geometrical parameter variations accurately without the need for the use of high-resolution grids. We expect this approach to be important for fast computational prototyping and optimization of practical photonic crystal and nanophotonic devices.

In the frequency domain the wave equation for the electric field is

$$(-\nabla \times \nabla \times + {k_0}^2 \epsilon_r)\mathbf{E} = \nabla \times \mathbf{M} + j\omega\mu_0\mathbf{J}, \qquad (1)$$

where ${k_0}^2 = \omega^2\epsilon_0\mu_0$ and $\mathbf{J}$ ($\mathbf{M}$) is the electric (magnetic) source current. To solve this equation we use a finite-difference frequency-domain method.[7] The fields are discretized on a nonuniform orthogonal grid truncated by a perfectly matched layer in its coordinate stretching formulation.[8] The equation for the field at each grid point involves only the fields at the six (four in two dimensions) adjacent grid points. Thus the resulting system matrix is sparse.

The system of linear equations resulting from discretizing Eq. (1) is of the general form

$$\mathbf{Z}(\mathbf{s})\mathbf{I} = \mathbf{V}, \qquad (2)$$

where $\mathbf{Z}$ is the system matrix, $\mathbf{s}$ is the vector of design parameters, $\mathbf{I}$ is the vector of unknown fields, and $\mathbf{V}$ is the source, which does not depend on $\mathbf{s}$ ($\nabla_s\mathbf{V} = 0$), since we focus on variations of the device structure. The response function of interest is a function of the field $T = T(\mathbf{I}(\mathbf{s}))$ and therefore has no explicit dependence on $\mathbf{s}$. The objective of the sensitivity analysis is to determine $\nabla_s T$. Using the AVM, one can show that[6]

$$\nabla_s T = -\hat{\mathbf{I}}^T(\nabla_s\mathbf{Z})\mathbf{I}, \qquad (3)$$

$$\mathbf{Z}^T\hat{\mathbf{I}} = [\nabla_{\mathbf{I}} T]^T, \qquad (4)$$

where $\mathbf{I}$, obtained from Eq. (2), is the vector of fields at the current design point and $\hat{\mathbf{I}}$ is the solution to the so-called adjoint problem [Eq. (4)]. In our case the matrix $\mathbf{Z}$ obtained from Eq. (1) is symmetric. Thus Eq. (4) requires that one determine the field when the source is the adjoint excitation $\hat{\mathbf{V}} = [\nabla_{\mathbf{I}} T]^T$, which is the gradient of the response with respect to the fields. As an example, if the response function is defined as the field intensity at a given monitor point, the adjoint excitation will be nonzero only at the monitor point.

A particularly efficient approach to solve Eqs. (2) and (4) is the use of a direct sparse matrix method that requires only a single LU decomposition of $\mathbf{Z}$ and two backsubstitutions. Having calculated $\mathbf{I}$ and $\hat{\mathbf{I}}$, we obtain the sensitivity with respect to any number of design parameters by calculating $\nabla_s\mathbf{Z}$, which has a negligible computational cost. Thus, when a direct solver is used, the only additional cost required for the sensitivity analysis is one backsubstitution for the solution of Eq. (4), which is typically at least an order of magnitude smaller than the cost of the LU decomposition.

In the device sensitivity analysis we are interested in the effects of variations of the dielectric function $\epsilon_r = \epsilon_r(\mathbf{r})$ on the response function of the device. To calculate the effect of varying the dielectric constant ϵ_{r1} of a particular device (assuming that the entire device region has the same dielectric constant ϵ_{r1}), it is straightforward to calculate $\nabla_s\mathbf{Z}$, and then, using

0146-9592/04/192288-03$15.00/0

Eq. (3), one obtains

$$\frac{\partial T}{\partial \epsilon_{r1}} = -{k_0}^2 \sum_i \hat{I}_i I_i \,, \tag{5}$$

where the summation is taken over the volume of this device.

In practice, it is particularly useful to determine the tolerance of the device performance to fabrication disorders. In this case we are interested in the effect of perturbations resulting from shifting of the interface between regions with different dielectric constants. Suppose that we have two regions with dielectric constants ϵ_{r1} and ϵ_{r2}. Since $\epsilon_r(\mathbf{r})$ is a step function, its derivative is a delta function, so the summation in Eq. (3) is limited to the interface between the two media. This surface summation needs to be carefully defined because of the discontinuity of the normal component of the electric field $E_\perp$ to the interface and was recently studied by Johnson *et al.*[9] in the context of perturbation theory. Following their approach, we showed that

$$\frac{\partial T}{\partial s} = -{k_0}^2 \sum_i \Delta {l_i}^{-1} \frac{\mathrm{d}h(\mathbf{r}_{\mathrm{surf}\,i}, s)}{\mathrm{d}s} \times [\Delta \epsilon_{12} \hat{E}_{\parallel i} E_{\parallel i} - \Delta({\epsilon_{12}}^{-1}) \hat{D}_{\perp i} D_{\perp i}], \tag{6}$$

where $\Delta\epsilon_{12} \equiv \epsilon_{r1} - \epsilon_{r2}$, $\Delta({\epsilon_{12}}^{-1}) \equiv {\epsilon_0}^{-2}({\epsilon_{r1}}^{-1} - {\epsilon_{r2}}^{-1})$, Δl_i is the local grid size normal to the interface, and the summation is taken over the interface. The function $h = h(\mathbf{r}_{\mathrm{surf}}, s)$ defined on the boundary surface is the distance that the interface between regions 1 and 2 shifts toward region 2. The summation in Eq. (6) is well defined, since both $E_\parallel$ and $D_\perp$ are continuous at the interface.

We focus on two-dimensional calculations as a proof of principle. For TE polarization we have $\mathbf{E} = E_z \hat{z}$ and the wave equation for the electric field becomes[8]

$$\left(\frac{\partial^2}{\partial x^2} + \frac{\partial^2}{\partial y^2} + {k_0}^2 \epsilon_r\right) E_z = j\omega\mu_0 J_z \,. \tag{7}$$

Similarly, for TM polarization we have $\mathbf{H} = H_z \hat{z}$ and

$$\left[\frac{\partial}{\partial x}\left(\frac{1}{\epsilon_r}\frac{\partial}{\partial x}\right) + \frac{\partial}{\partial y}\left(\frac{1}{\epsilon_r}\frac{\partial}{\partial y}\right) + {k_0}^2\right] H_z = j\omega\epsilon_0 M_z \,. \tag{8}$$

In the TM case, $\mathbf{I}$ and $\hat{\mathbf{I}}$ correspond to magnetic fields. To use Eq. (6) where the sensitivity is calculated in terms of the electric field, we first solve Eq. (8) to determine H_z, from which $E_\parallel$ and $D_\perp$ can then be calculated. The adjoint problem can also be recast in terms of the magnetic field. If the response function is defined as $T = |H_{\mathrm{obs}}|^2$, where H_{obs} is the field at the observation point, we can show that the adjoint source is $\widehat{M}_z = (-2/j\omega\mu_0){H_{\mathrm{obs}}}^*$ at the observation point and zero elsewhere.

To validate our method, we compare it with the direct approach (DA),[6] in which sensitivity is simply calculated as

$$\frac{\partial T}{\partial s} \simeq \frac{T(s + \Delta s/2) - T(s - \Delta s/2)}{\Delta s} \,. \tag{9}$$

We choose a high-resolution grid (160 points per a, where a is a length used for normalization). In Fig. 1(a) we show the sensitivity of the response function, calculated with the DA and our method for the structure shown in the inset of Fig. 1. We observe that there is excellent agreement over the entire frequency range.

Since our method uses a perturbative approach for the calculation of sensitivity, we expect it to be accurate even when a low-resolution grid is used. To verify this, we compare our method in a low-resolution grid (16 points per a) with the benchmark DA in the high-resolution grid (160 points per a). Results are shown in Fig. 1(b) for the sensitivity with respect to object size. The agreement is very good over the entire frequency range in spite of the 10 times coarser grid. In Fig. 1(b) we also show the result obtained by the DA in the low-resolution grid. We observe that the DA, when applied to a low-resolution grid, introduces very large error especially at high frequencies.

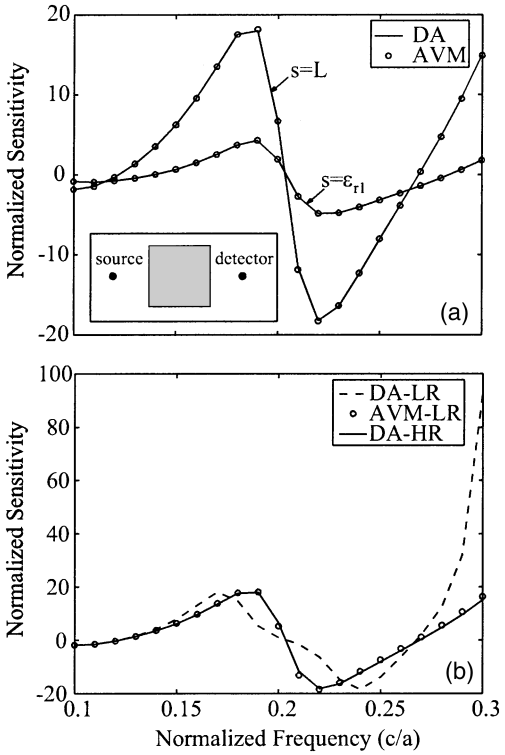

Fig. 1. (a) Comparison of the DA and AVM methods in high-resolution grids (160 points per a). We show the normalized sensitivity of the transmission defined as $\partial T/\partial s(T/s)^{-1}$ (s is either the square size L or ϵ_{r1}) as a function of frequency. The structure, a dielectric block, is shown in the inset, $L = 0.9375a$, and $\epsilon_{r1} = 11.56$. (b) Comparison of the DA and AVM methods in low-resolution grids (16 points per a) with the benchmark DA in the high-resolution grid (160 points per a) for $s = L$.

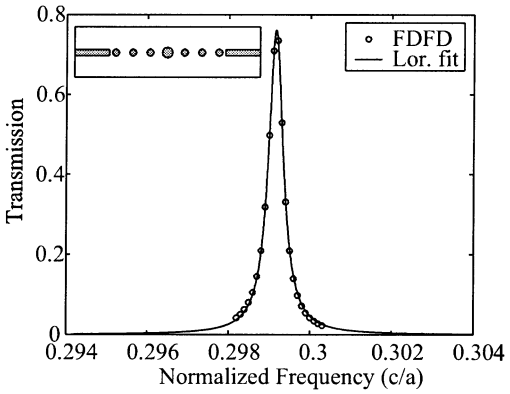

Fig. 2. Transmission spectrum calculated by the finite-difference frequency-domain (FDFD) method and the corresponding Lorentzian fit for a photonic-crystal-based bandpass optical filter (the device geometry is shown in the inset). The distance between adjacent rods is a, and their radius is $0.2a$. The radius of the central dielectric rod is $r_d = 0.4a$. The width of the dielectric waveguides is $0.35a$, and their distance from the center of the closest rod is $0.4a$.

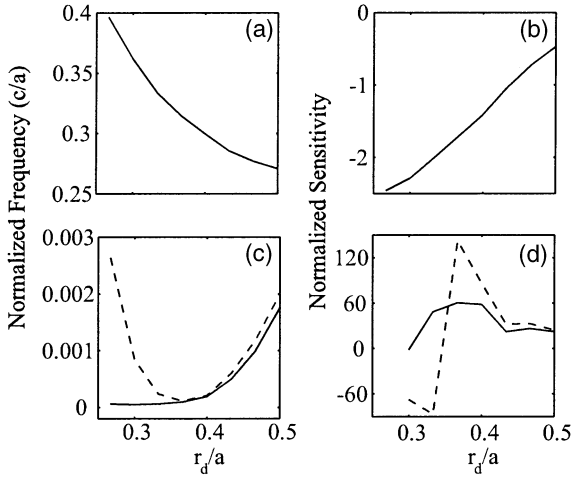

Fig. 3. (a) Ω_0, (c) Ω_1, Ω_2 (dashed curve) as a function of the radius of the central dielectric rod r_d. Normalized sensitivities (b) $\partial\Omega_0/\partial r_d(\Omega_0/a)^{-1}$, (d) $\partial\Omega_1/\partial r_d(\Omega_1/a)^{-1}$, $\partial\Omega_2/\partial r_d(\Omega_2/a)^{-1}$ (dashed curve) as a function of r_d.

As an application of our method, we calculate the sensitivity of the resonant frequency and the bandwidth of an optical filter[10] shown in the inset of Fig. 2. The transmission spectrum of such a device close to the resonant frequency can be very well approximated by a Lorentzian shape

$$T(\omega) = \frac{{\Omega_1}^2}{(\omega - \Omega_0)^2 + {\Omega_2}^2}, \tag{10}$$

as shown in Fig. 2, where Ω_0 is the resonant frequency and Ω_1 and Ω_2 are bandwidths.

To calculate $\partial\Omega_0/\partial s$, $\partial\Omega_1/\partial s$, and $\partial\Omega_2/\partial s$, we differentiate Eq. (10) to obtain

$$\frac{\partial T(\omega_i)}{\partial s} = \frac{\partial T(\omega_i)}{\partial \Omega_0}\frac{\partial \Omega_0}{\partial s} + \frac{\partial T(\omega_i)}{\partial \Omega_1}\frac{\partial \Omega_1}{\partial s} + \frac{\partial T(\omega_i)}{\partial \Omega_2}\frac{\partial \Omega_2}{\partial s}. \tag{11}$$

Here $\partial T(\omega_i)/\partial s$ is calculated using the method described above. In addition, $\partial T(\omega_i)/\partial\Omega_0$, $\partial T(\omega_i)/\partial\Omega_1$, and $\partial T(\omega_i)/\partial\Omega_2$ can be analytically calculated from Eq. (10), once the transmission spectrum is fitted with a Lorentzian. Thus, one can determine $\partial\Omega_0/\partial s$, $\partial\Omega_1/\partial s$, and $\partial\Omega_2/\partial s$ accurately by applying Eq. (11) to at least three frequencies and by solving the overdetermined system in the least-squares sense. Alternatively, $\partial\Omega_0/\partial s$, $\partial\Omega_1/\partial s$, and $\partial\Omega_2/\partial s$ can be obtained if we differentiate some other function of the transmission spectrum such as T^{-1}. Depending on the design point, either $\partial T(\omega_i)/\partial s$ or $\partial T^{-1}(\omega_i)/\partial s$ results in a better least-squares fit. In each case we use the one that provides the best fit to our results.

In Figs. 3(a) and 3(c) we show the calculated Ω_0, Ω_1, and Ω_2 for the device structure of Fig. 2 as a function of the radius of the central dielectric rod, r_d. The calculated Ω_0, Ω_1, and Ω_2 are consistent with previously published results.[10] In Figs. 3(b) and 3(d) we show the calculated sensitivities of Ω_0, Ω_1, and Ω_2. We observe that Ω_1 and Ω_2 are much more sensitive to variations in r_d than is Ω_0. The calculated sensitivities are consistent with the values obtained by the DA in the same grid.

This research was supported by the Defense Advanced Research Projects Agency/Microelectronics Advanced Research Corporation under the Interconnect Focus Center. S. Fan's e-mail address is shanhui@stanford.edu.

References

1. K.-C. Kwan, X. Zhang, Z.-Q. Zhang, and C. T. Chan, Appl. Phys. Lett. **82,** 4414 (2003).
2. A. Chutinan and S. Noda, J. Opt. Soc. Am. B **16,** 240 (1999).
3. Z.-Y. Li and Z.-Q. Zhang, Phys. Rev. B **62,** 1516 (2000).
4. A. A. Asatryan, P. A. Robinson, L. C. Botten, R. C. McPhedran, N. A. Nicorovici, and C. M. de Sterke, Phys. Rev. E **62,** 5711 (2000).
5. S. Fan, P. R. Villeneuve, and J. D. Joannopoulos, J. Appl. Phys. **78,** 1415 (1995).
6. N. K. Georgieva, S. Glavic, M. H. Bakr, and J. W. Bandler, IEEE Trans. Microwave Theory Tech. **50,** 2751 (2002).
7. S. D. Wu and E. N. Glytsis, J. Opt. Soc. Am. A **19,** 2018 (2002).
8. J. Jin, *The Finite Element Method in Electromagnetics* (Wiley, New York, 2002).
9. S. G. Johnson, M. Ibanescu, M. A. Skorobogatiy, O. Weisberg, J. D. Joannopoulos, and Y. Fink, Phys. Rev. E **65,** 066611 (2002).
10. S. G. Johnson, S. Fan, A. Mekis, and J. D. Joannopoulos, Appl. Phys. Lett. **78,** 3388 (2001).